Journal of the European Ceramic Society 13 (1994) 159–166

Surface Toughening of Liquid Phase Sintered Silicon Carbide by Surface Nitridation

Peter Greil,* Hans Georg Bossemeyer, Andrea Klüner

Technical University of Hamburg Harburg, Advanced Ceramics Group, Hamburg Germany

&

Jiang Dongliang, She Jihong

Shanghai Institute of Ceramics, Chinese Academy of Science Shanghai, China

(Received 3 May 1993, revised version received 27 July 1993, accepted 10 September 1993)

Abstract

The formation of thin sialon surface layers on liquid phase sintered silicon carbide containing Al_2O_3 and Y_2O_3 during post hot isostatic pressing in N_2 atmosphere was examined. At a N_2 pressure of 200 MPa multiphase reaction layers were growing with parabolic kinetics at 1750 C. The surface reaction layer is composed of β'-$Si_{6-z}Al_zO_zN_{8-z}$ ($z = 1.6$–3.3) as the major phase and additional oxynitride phases. Based on an indentation method an apparent fracture toughness was measured from which residual stresses in the surface layer were derived. Large compressive stresses up to several hundred MPa were estimated in very thin sialon layers ($d_1 < 10\,\mu m$) which have a potential for protection against impact wear and ultimate failure of SiC components even of complex shape.

Es wurde die Bildung von dünnen Sialonschichten auf der Oberfläche von flüssigphasengesintertem Siliziumcarbid, das Al_2O_3 und Y_2O_3 enthielt, während nachträglichem Heißpressen in N_2-Atmosphäre untersucht. Bei einem N_2 Druck von 200 MPa bildeten sich mehrphasige Reaktionsschichten, deren kinetisches Verhalten bei 1750 C parabolisch war. Die Oberflächenreaktionsschicht besteht hauptsächlich aus β' $Si_{6-z}Al_zO_zN_{8-z}$ ($z = 1.6$–3.3), zusätzlich enthält sie Oxynitrid. Basierend auf der Eindruckmethode wurde ein Rißwiderstand gemessen, von dem Restspannungen in der Oberflächenschicht abgeleitet wurden. Große Druckspannungen bis zu mehreren hundert MPa wurden in sehr dünnen Sialonschichten ($d_1 < 10\,\mu m$) abgeschätzt. Diese Schichten bieten eine Möglichkeit des Schutzes gegenüber Stoßverschleiß und Versagen von SiC Keramiken sogar bei komplexen Formen.

On a étudié la formation de couches minces de sialon à la surface de carbure de silicium (contenant Al_2O_3 et Y_2O_3 frittés avec une phase liquide) lors de pressages à chaud sous atmosphère de N_2. A une pression de 200 MPa de N_2, des couches multiphasées croissent avec une cinétique parabolique à 1750 C. La couche formée en surface est composée de β' $Si_{6-z}Al_zO_zN_{8-z}$ ($z = 1.6$–3.3) en majorité, et de phases oxynitrures. A partir d'expériences d'indentation, nous avons mesuré la résistance apparente à la fracture d'où ont été déduites les contraintes résiduelles dans la couche de surface. Ces estimations conduisent à des contraintes importantes, atteignant quelques centaines de MPa dans les couches de sialon très fines ($d_1 < 10\,\mu m$), ceci pourrait permettre la protection de composants en SiC, même s'ils sont de forme compliquée, contre l'usure due aux couches et la rupture.

1 Introduction

Nitridation of dense SiC ceramic components to form layered SiC/Si_3N_4 composite materials may offer an attractive way to improve surface-sensitive mechanical properties of complex-shaped SiC components. Thus, surface strengthening of SiC ceramics was obtained by annealing in an NH_3 atmosphere of ambient pressure at temperatures of 400–900°C[1] or in a N_2 atmosphere of high pressure at temperatures above 1700°C.[2] Thermodynamic

* Present address: Glass and Ceramics Department, University of Erlangen Nuernberg, Erlangen, Germany

Journal of the European Ceramic Society 0955-2219/94/$7.00

evaluation of the phase stabilities in Si_3N_4/SiC composite materials suggests that SiC will become unstable in a N_2 atmosphere of high pressure and should be nitrided according to[3,4]

$$3\alpha\text{-SiC(s)} + 2N_2(g) \rightarrow \beta\text{-}Si_3N_4(s) + 2C(s) \quad (1)$$

At 1750°C the equilibrium N_2 pressure for reaction (1) is approximately 3·8 MPa[5,6] so that under usual hot-isostatic pressing conditions with temperatures above 1750°C and gas pressure above 10 MPa Si_3N_4 should form on the surface of SiC. Reaction (1) seems to be facilitated in the presence of liquid phases in the grain boundaries of SiC. For example, post-hot isostatic pressing of dense SiC doped with 3 wt% Al_2O_3 at 1850°C with a N_2 pressure of 200 MPa resulted in the formation of Si_3N_4 surface layers with a thickness ranging from 5 to 15 μm.[2] A substantial increase of bending strength from 660 MPa of the SiC up to more than 1000 MPa of the SiC/Si_3N_4 layer composite was observed, which was attributed to the generation of thermally induced compressive stresses[7,8] in the Si_3N_4 surface layer during cooling from nitridation temperature. While residual stresses in surface films can cause substrate fracture and component failure,[9] surface toughening due to compressive stresses is expected to be protective against component failure from incidental contacts with particulate matters.[10] The magnitude of the misfit stresses primarily depends on the cooling conditions and the elastic and thermal properties of the surface layer and the substrate material.[11] Thus, investigation of formation and growth kinetics of the Si_3N_4 surface layer appears to be a fundamental requirement in order to optimize in-situ surface toughening associated with the formation of thin nitride layers on the surface of SiC compacts even of complex geometry.

It is the aim of the present work to analyze the kinetics of nitride layer growth on the surface of hot-pressed α-SiC doped with Al_2O_3 and Y_2O_3. Specimens with different surface layer thickness were prepared by variation of the post hot isostatic pressing conditions. Elemental distribution near the specimen surface was measured by EDX and phase composition by XRD. The magnitude of residual stresses in the nitrided surface layers was derived by means of an indentation method.

2 Experimental Procedure

Powder mixtures of submicron α-SiC (FCP 06, Sika, Arendal Smeltwerk a.s., Eydenhavn, Norway) containing 6·85 wt% Y_2O_3 (H.C. Starck, Berlin, Germany) and 5·15 wt% Al_2O_3 (CT 8000 SG, Alcoa, Pittsburgh, PA, USA) were prepared by attrition milling in ethanol for 4 h. The three powders are characterized by a low chemical impurity content and high specific surface areas of 15 m^2/g, 17 m^2/g, and 15 m^2/g, respectively, Table 1. The molar composition of the oxidic sintering additives corresponds to 3 Y_2O_3 5 Al_2O_3 in order to allow precipitation of crystalline $Y_3Al_5O_{12}$ (YAG) from the intergranular liquid phase upon cooling.[12] After drying at 110°C for 24 h at $p \approx 10^3$ Pa the powder mixture was filled into BN coated graphite dies and hot-pressed to cylindrical pellets with a diameter of 35 mm and a thickness of 6 mm. The hot-pressing temperature of 1750°C was kept constant for 30 min and the atmosphere was N_2 at 0·1 MPa. After hot-pressing density was measured according to the Archimedian principle. Fractional density was higher than 97% of theoretical density, indicating that no open porosity remained.

Table 1. Characteristics of SiC powder

Chemical composition (weight %)			
Crystalline SiC	97·8	Fe	0·01
Free SiO_2	1·5	Al	0·005
Free Si	0·09	Ti	0·01
Free C	0·5	Ca	0·002
O	0·9	F	0·02

Mean grain size (sedigraph) 0·6 μm
Specific surface area (BET) 15 m^2/g

The hot-pressed specimens were diamond ground and polished to 1 μm to assure a reproducible surface finish. Specimens were post hot isostatically pressed first in Ar to increase fractional density to 99% and subsequently in N_2 atmosphere to form the reaction layer. N_2 pressures of 8 MPa, 50 MPa and 200 MPa and temperatures of 1600°C, 1750°C and 1900°C were chosen. The reaction temperature was kept constant for 30 min, 60 min and 120 min, respectively. From the post-hot isostatically pressed pellets specimens were prepared for microscopic (SEM and LM) measurement of the nitride layer thickness according to standard procedures. In addition to the optical analysis nitride layer thickness was determined from elemental point analysis (5 × 20 μm) data using EDX with an ultrathin Be window. Crystalline phase composition of the reaction layer was analyzed by X-ray diffraction using monochromated Cu-K_α radiation. The composition of the β′ sialon solid solution phase was determined from lattice constant measurements[13] using the (100), (110), (200), (300), (002) and (410) peaks.

Residual stresses that develop in the surface layer upon cooling were determined by measuring the apparent critical stress intensity factor at the surface of nitrided specimens using the indentation technique developed by Evans & Charles.[14] A controlled crack pattern was introduced into the uncoated and the coated (surface nitrided) specimens by means of

a Vickers indenter. Assuming that the coating layer influences the indentation pattern by virtue of its stress state but not by its fracture properties the residual stress in a surface layer parallel to the free surface, σ_1, is approximated by[10,15]

$$\sigma_1 \approx \frac{1}{2\psi\sqrt{d_1}}(K^0 - K^*) \qquad (2)$$

where K^0 is the critical stress intensity factor for the uncoated, stress free SiC material and K^* is the apparent toughness of the SiC coated with a thin nitride layer of thickness d_1. ψ is a geometrical constant which for small surface cracks of half penny shape attains $1{\cdot}29 \pm 0{\cdot}2$.[16] K^0 and K^* were derived from the radii of the surface cracks, c, produced by an indentation load, P, on the surface of the uncoated and coated specimens, respectively[17]

$$K = \aleph P c^{-3/2} \qquad (3)$$

where $\aleph$ is a dimensionless field intensity parameter which is given as a function of elastic modulus, E, and hardness, H,[18]

$$\aleph = (0{\cdot}016 \pm 0{\cdot}004)(E/H)^{1/2} \qquad (4)$$

For SiC, $E = 430$ GPa and $H = 26$ GPa so that $\aleph = 0{\cdot}065 \pm 0{\cdot}016$. Indentations were made using a Vickers diamond pyramid at loads of 30, 50 and 100 N and only well-developed radial crack patterns were taken into account (i.e. $c > 2{\cdot}5a$ where a is the half diagonal of the contact zone (hardness)). Indentations were made in air with a load hold of 10 s and crack lengths were measured 2 min after unloading.

3 Results and Discussion

3.1 Nitride layer composition

Thickness and phase composition of the nitride surface layers generated under various pressure, temperature and time conditions are summarized in Table 2. While in the hot pressed SiC material

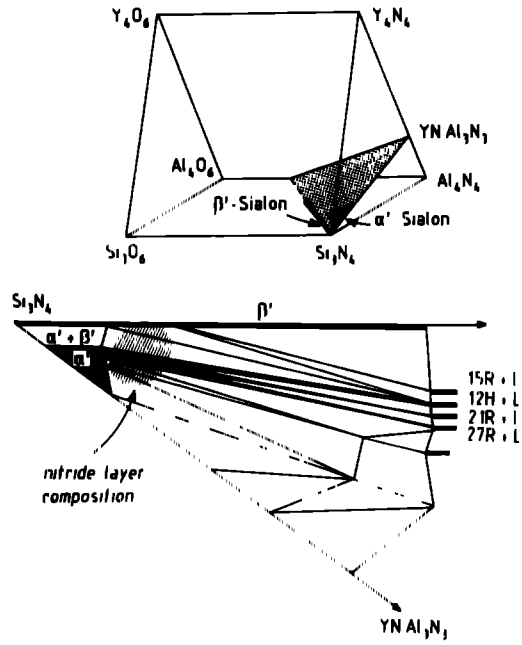

Fig. 1 Jaenecke prism of the Y–Si–Al–O–N system and part of the compositional plane $Y_4(Si,Al)_{12}(N,O)_{16}$ with the phase relations at 1750 °C/87 Sla and the tentative location of the nitride layer composition (see text)

$Y_3Al_5O_{12}$ was found as the only secondary crystalline phase located in the grain boundaries, a multiphase microstructure is formed in the nitride reaction layers. β-Si_3N_4 solid solution (β' sialon) is the major phase formed by substitution of Si^{4+} and N^{3-} by Al^{3+} and O^{2-} in the β-Si_3N_4 lattice.[14] From the lattice constants a_0 and c_0 the compositional parameter z in β' $Si_{6-z}Al_zO_zN_{8-z}$ was determined as $z \approx 1{\cdot}6$–$3{\cdot}3$.[19] The solid solution composition was found to vary with layer thickness d_1 from $z = 3{\cdot}3$ at $d_1 = 2\,\mu$m (No. 1) to an almost constant composition with $z = 1{\cdot}6$–$1{\cdot}8$ at $d_1 = 11$–$23\,\mu$m (Nos. 3–7), Table 2.

Incorporation of Y^{3+} into the silicon nitride lattice stabilizes α-Si_3N_4 solid solution (α'-Sialon, α' $Y_xSi_{12-(m+n)}Al_{(m+n)}O_nN_{16-n}$ with $x = 0{\cdot}33$–$0{\cdot}67$, $m = 1$–4 and $n = 0$–$2{\cdot}5$)[20] which can exist in equilibrium with β' sialon in the Si_3N_4 rich part of the quinary Si–Y–Al–O–N system.[21] Figure 1 represents a section of the three dimensional Jaenecke prism (Si_3N_4–AlN–Al_2O_3–SiO_2–Y_2O_3–YN) with

Table 2. Thickness and phase composition of nitride surface layers formed at various post hot isostatic pressing conditions

Number	*Reaction conditions*			d_1 (μm)	*Phase composition*	
	T (°C)	P_{N_2} (MPa)	*t* (h)		(β')	*Minor phases*
1	1600	200	1	2.0 ± 0.9	3.3	YAG
2	1750	8	1	2.2 ± 1.1	3.1	YAG, 12H
3	1750	50	1	12 ± 5	1.6	α', YAG, 12H
4	1750	200	0.5	11 ± 3	1.8	α', YAG
5	1750	200	1	13 ± 4	1.7	α', $Y_2Si_2O_7$
6	1750	200	2	23 ± 6	1.7	α', AlN
7	1900	200	1	32 ± 6		α', AlN

β', α' Solid solution phases of Si_3N_4 (see text); YAG, $Y_3Al_5O_{12}$; 12H, $SiAl_4O_2N_4$

the major condensed phase relations in the silicon nitride rich part of the α′-sialon plane at 1750°C [22] The tentative location of the nitride layer composition as derived from the results of XRD analysis is shown as a shaded area. 12 H, 15 R, 21 R and 27 R are Si and O containing polytypes of AlN [23] which form various multiphase equilibria with the Si_3N_4 solid solution phases and an additional oxynitride liquid phase L. $Y_2Si_2O_7$ crystallizes from an Y-containing oxynitride liquid phase [24]

Figure 2 shows a SEM micrograph of the sialon layer which was formed after 2 h at 1750°C and a N_2 pressure of 200 MPa (No. 6) The elongated β′ sialon crystals (dark) have preferentially grown with their columnar axis perpendicular to the surface and the Y-containing secondary phases (bright) are located at the grain boundaries Preferential orientation of the β′-sialon phase due to anisotropic growth of hexagonal crystals in [001] has also been confirmed by X ray analysis which revealed a pronounced increase of (002)/(*hk*0) intensity ratios at high reaction layer thickness. Measurements of the elemental distribution of specimen No. 4 nitrided for 30 min at the same temperature and pressure are given in Fig. 3 The formation of the nitride layer is confirmed by a high N concentration which suddenly drops beyond approximately 10–15 μm. This

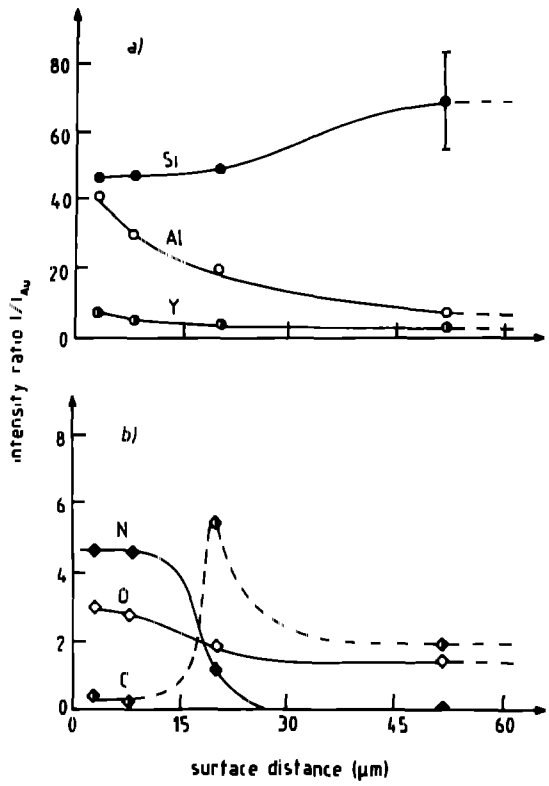

Fig. 3. Element distribution in the SiC nitrided at 1750°C for 30 min with a nitrogen pressure of 2000 MPa (No 4) as a function of surface distance measured by EDX. (a) Cations (b) anions

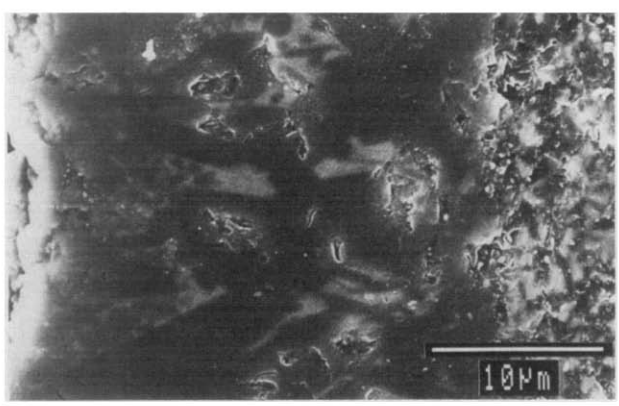

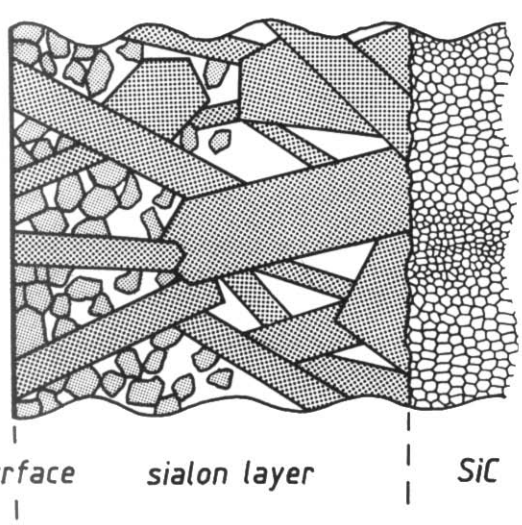

Fig. 2. SEM micrograph of the sialon surface layer formed after 2 h at 1750°C with a nitrogen pressure of 200 MPa (No. 6)

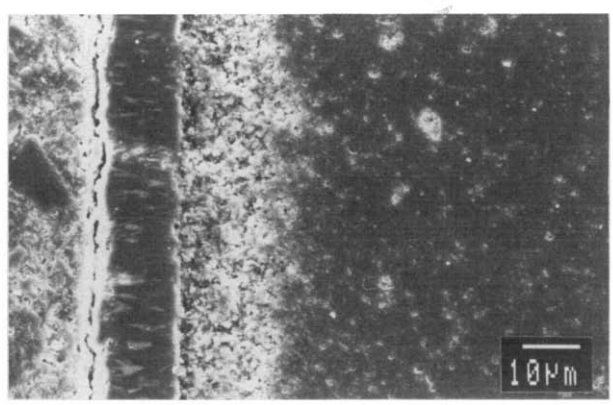

(a)

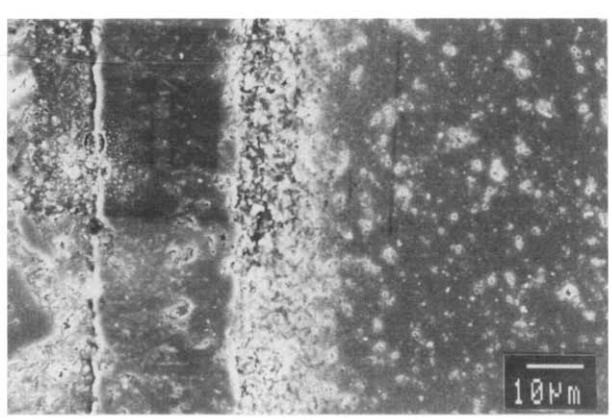

(b)

Fig. 4. SEM micrographs of nitride layers formed at 1750°C with a nitrogen pressure of 200 MPa for (a) 30 min (No 4) and (b) 120 min (6)

coincides well with the optically measured thickness of the reaction layer. A clear tendency of increasing Al and O concentration near the outer layer surface can be seen, which is attributed to the dissolution of these elements in the β' sialon solid solution phase. Calculation of heterogeneous phase equilibria in the SiAlON system have shown the high stability of β' sialon with $z \approx 4$ under similar temperature and pressure conditions.[7] Assuming all alumina from the SiC material to be dissolved in β' sialon only a value of $z \approx 0.26$ would be possible. Thus, an increase of substitution level z in the β'-sialon phase requires diffusion of Al and O from the bulk into the growing reaction layer.

In contrast to the bulk, only traces of C could be found in the nitride layer. At the nitride/carbide layer, however, a pronounced C peak indicates an enrichment of C ahead of the growth front where a zone of high porosity was observed, Fig. 4. While in the oxygen free Si–N–C system Si_3N_4 is in equilibrium with SiC and solid C at the interface boundary, in the oxide containing system Si–N–C–O solid Si_2N_2O may be in equilibrium with SiC and Si_3N_4, whereas gaseous CO and SiO are major constituents of the gaseous phase.[3] Thermodynamic calculations in the system Si–Al–Y–N–C–O have shown similar relationships, with the exception of β' sialon being the stable phase instead of β-Si_3N_4.[26] Thus, the high porosity found at the nitride/carbide interface is to be attributed to the formation of gaseous reaction products, suggesting

$$(6-z)SiC + 2Al_2O_3 + \left[\frac{8-z}{2}\right]N_2 \rightarrow \beta' Si_{6-z}Al_zO_zN_{8-z} + \left[\frac{12-3z}{2}\right]C + \frac{z}{2}CO \quad (5)$$

as the dominating reaction and additional formation of Y containing α' sialon and AlN polytypes. The nitride reaction layer acts as barrier layer for carbon which explains the very low carbon content found in the reaction layer and the enrichment of C in the porous interface layer in front of the reaction layer, Fig. 3.

3.2 Nitride layer thickness

Thickness of the nitrided surface layer was found to vary strongly with temperature and time of post-hot isostatic pressing, whereas at the high N_2 pressures the layer thickness remains almost unaffected by change of pressure, Table 2. As can be seen in Fig. 4 mean nitride layer thickness increased from approximately 11 μm after 30 min to 23 μm after 120 min post-hot isostatic pressing at 200 MPa and 1750°C. Figure 5 shows time dependence of the nitride layer thickness at a N_2 pressure of 200 MPa at different temperatures. The data at 1750°C can be fitted by a

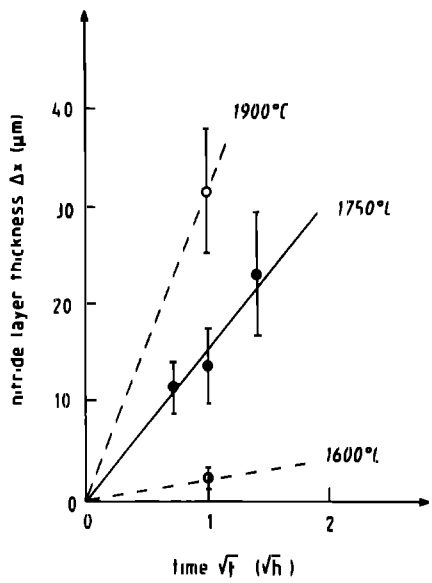

Fig. 5. Growth kinetics of nitride surface layer at a constant nitrogen pressure of 200 MPa.

linear relation between layer thickness d_1 and square root of time $\sqrt{t}$:

$$d_1 = (\gamma t)^{1/2} \quad (6)$$

From the parabolic rate equation a growth mechanism controlled by diffusion through the nitride reaction layer can be concluded which obeys Fick's diffusion law.[27] In spite of the lack of reliable diffusion data for sialon phases data for diffusivities of metals and C or N in a variety of ceramic carbides and nitrides[28] suggest that Si or Al diffusivity should be significantly slower compared to N or O, respectively. Hence, growth rate of the nitride layer is likely to be governed by the inward diffusion of nitrogen from the outer solid/gas interface to the inner nitride/carbide interface. The diffusion coefficients for volume (bulk) diffusion of nitrogen in β-Si_3N_4 at normal pressure are $D_V^N = 1.4 \times 10^{-13}$ cm^2/s, 5.7×10^{-14} cm^2/s and 1.4×10^{-12} cm^2/s for temperatures of 1600°C, 1750°C and 1900°C, respectively.[29] For the rate constant γ ($\approx D_{eff}$) values of 1.09×10^{-11} cm^2/s, 6.25×10^{-10} cm^2/s and 2.8×10^{-9} cm^2/s were calculated from eqn (6). From the temperature dependence of the rate constant α ($= \alpha_0 \exp(-Q/RT)$) an apparent activation energy of 630 kJ/mol was derived from an Arrhenius relation. This is substantially lower compared to 780 kJ/mol for lattice diffusion of nitrogen in β-Si_3N_4.[29] Neglecting the influence of the pressure on the diffusivity due to the negligible contribution of excessive volume on the activation energy term in this system[30] lattice diffusion of nitrogen cannot explain the growth kinetics of the nitride layer. Accelerated material transport via the grain boundaries, however, results in significantly higher growth rates. For the ratio of grain boundary to volume (lattice) diffusion coeffi

cients, D_{gb}/D_v, a ratio of $\cdot 10^5$ is a reasonable lower boundary for a variety of polycrystalline nitrides [31]. Thus, for [32]

$$D_{eff} \approx D_v\left(1 + \frac{\delta}{G}\frac{D_{gb}}{D_v}\right) \quad (7)$$

an effective diffusion coefficient $D_{eff} \approx (10^2\text{–}10^3) \times D_v$ results for reasonable values of grain boundary width $\delta = 1\text{–}10$ nm and grain size $G = 1\text{–}10\,\mu$m, which is in the range of the experimentally observed values for γ.

3.3 Residual surface layer stresses

Figure 6 shows the indentation patterns of the uncoated and the surface nitrided SiC (No. 4). In contrast to the well-developed crack pattern on the surface of the uncoated SiC, no indentation cracks can be seen on the surface of the nitrided SiC sample, even though dark-field imaging light microscopy reveals indentation cracks of significantly reduced lengths. Figure 7 shows the apparent fracture toughness K^* versus layer thickness d_l as derived from Vickers indentation measurements. While the uncoated SiC material is characterized by

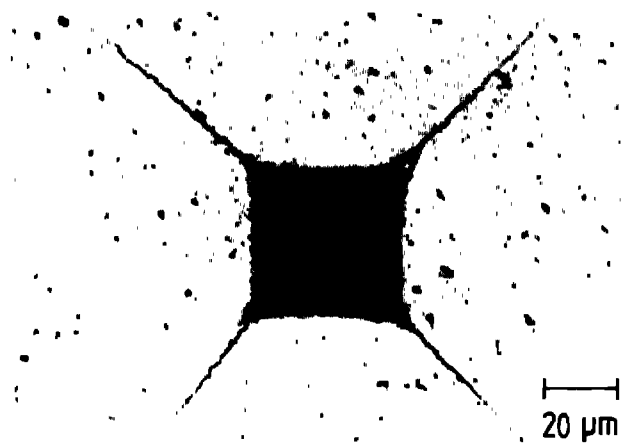

(a)

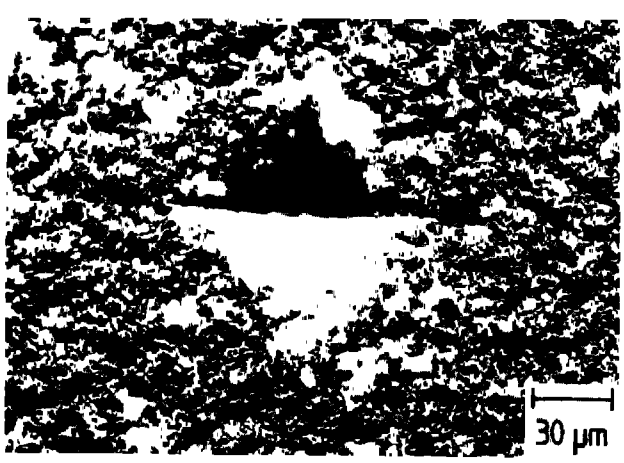

(b)

Fig. 6. Light optical micrographs of Vickers indentations (50 N) on the surface of (a) uncoated and (b) nitrided SiC specimen No. 4.

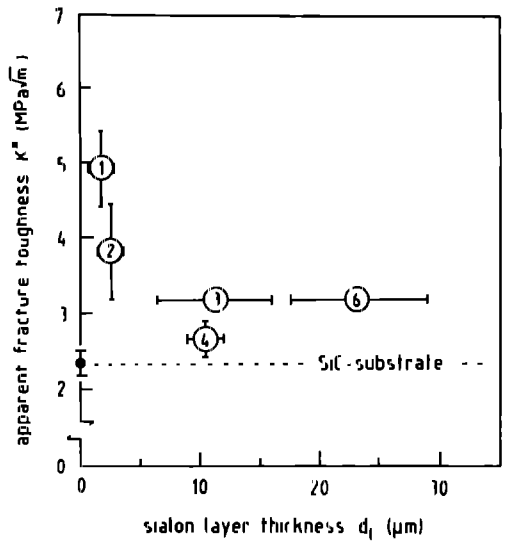

Fig. 7. Apparent fracture toughness K^* measured by indentation of the surface nitrided specimens.

$K^0 = 2{\cdot}3 \pm 0{\cdot}6\,\mathrm{MPa}\sqrt{\mathrm{m}}$, apparent fracture toughness K^* attains significantly higher values for all specimens coated with sialon layers, suggesting the presence of residual stresses [10]. Apparent toughness fell rapidly with increasing layer thickness beneath the surface from $K^* = 5\,\mathrm{MPa}\sqrt{\mathrm{m}}$ at $d_l = 2\,\mu$m to a steady value close to $3\,\mathrm{MPa}\sqrt{\mathrm{m}}$ at $d_l \cdot 10\,\mu$m. A similar dependence of apparent fracture toughness on the distance from the surface was observed in surface-toughened sialon ceramics where the surfaces were grit blasted with high velocity Al_2O_3 particles [33]. The residual stresses derived from K^* measurements are given in Fig. 8. Although absolute values of the experimentally derived stresses may significantly deviate from the real stress state, due to idealized assumptions for stress/strain distribution and crack pattern development in the layer and at the layer/substrate boundary,[10] the relative stress variation indicates decreasing residual layer stresses with increasing thickness.

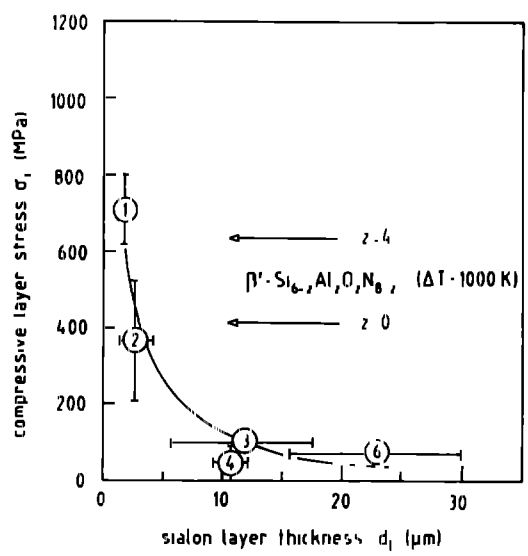

Fig. 8. Compressive residual stresses in the nitrided surface layers calculated from eqn (2).

The observed variation may be related to systematic changes of the coating layer microstructure, i.e. thickness and porosity at the nitride/carbide interface and the layer composition. Tailoring of the nitride layer microstructure by controlling the layer growth kinetics and variation of the additive content in the SiC base material therefore allows a systematic change of the reaction layer properties which have a strong impact on the surface stress formation. With increasing z, for example, grain shape and size were found to change from submicron sized grains of round shape to needle like crystals with grain sizes in the range of 1–10 μm.[34] In particular elastic properties and thermal expansion mismatch between the nitride layer and the SiC substrate ($\alpha_s = 4.35 \cdot 10^{-6}$/K from room temperature to 1000°C) strongly affect the residual misfit stress in the surface layer, σ_1, which will be generated upon cooling through ΔT:[11]

$$\sigma_1 = \frac{E_1(\alpha_s - \alpha_1)\Delta T}{1 - \nu_1} - f(d_1, E_1) \qquad (8)$$

where $f(d_1, E_1)$ is a function of layer to substrate thickness and layer to substrate elastic properties which, for the case of very thin layers, equals unity. With increasing Al and O substitution in β' sialon e.g. from $z = 0$ to $z = 4.2$, the mean linear thermal expansion coefficient decreases from $\alpha_1 = 3.4 \cdot 10^{-6}$/K to $2.4 \cdot 10^{-6}$/K[35] and the elastic modulus from $E_1 = 310$ GPa to 235 GPa,[36] respectively. Thus, for $\Delta T = 1000$°C and $\nu_1 = 0.28$ (Poisson ratio)[37] maximum residual compressive stresses of 410 MPa and 640 MPa are calculated from eqn (8) for β-Si_3N_4 ($z = 0$) and β' sialon ($z = 4$) layer compositions. As may be seen from Fig. 8, compressive stresses of the same magnitude were derived from measurements of indentation crack lengths.

Due to the complex multiphase microstructure of the sialon layer, however, the misfit stresses calculated according to eqn (8) can only be taken as a first approximation to indicate the tendency of stress variation with change of nitride layer composition and microstructure. With increasing nitride layer thickness the pronounced texture of the needle like sialon grains may significantly affect the crack propagation in the coating layer and hence the apparent fracture toughness of the coated material. Due to the lower amount of residual intergranular glassy phase in the sialon layers[34] stress relaxation processes may be reduced, resulting in higher freezing temperatures[38] and hence higher surface stresses than in glassy phase containing layers. In the case of gradient compositional change in the nitride layer, as may be expected from the experimental results, Fig. 3, the large stress gradients near the nitride/carbide interface (layer under compression and substrate under tension) should be reduced, which may result in improved adhesion strength of the reaction layers.

4 Conclusions

Dense layers of a multiphase sialon composition may be formed on the surface of SiC ceramics sintered with Al_2O_3 and Y_2O_3 by post hot isostatic pressing in N_2 atmosphere. Layer growth at an intermediate stage is likely to be dominated by inward diffusion of nitrogen, whereas Al, Y and O are transported from the bulk into the nitride layer to form sialon phase(s). Variation of the layer composition can be used to tailor the properties of the surface layer which have a strong impact on the development of compressive surface stresses.

For practical use very thin surface reaction layers with a thickness less than 10 μm seem to be of a particular interest for surface toughening, which can be formed under moderate temperature (1600°C) and N_2 pressure (< 10 MPa) conditions. The sialon layers of low thickness and high residual stresses are expected to be protective against erosion wear and ultimate failure of ceramic components. Thus, in situ formation of thin sialon layers provides an interesting possibility for improving the mechanical properties of complex shaped SiC components without the necessity of mechanical surface finishing.

Acknowledgement

The Deutsche Forschungsgemeinschaft and Academia Sinica are acknowledged for financial support of this work under Gr 961/7-1. The authors are grateful to Juergen Roedel for helpful discussions.

References

1. Arahori, T. & Iwamoto, N. Surface nitridation of silicon carbide ceramics. *J. Ceram. Soc. Jpn (Int. Edn)* **97** (1989) 1347.
2. Jiang, D. L., She, J. H., Tan, S. H. & Greil, P. Strengthening of silicon carbide ceramics by surface nitridation during hot isostatic pressing. *J. Am. Ceram. Soc.*, **75** (1992) 2568.
3. Wada, H., Wang, M. J. & Tien, T. Y., Stability of phases in the Si-C-N-O system. *J. Am. Ceram. Soc.* **71** (1988) 837.
4. Watori, K. & Ishizaki, K., Influence of gas pressure on HIP sintered silicon nitride and stability of carbon impurity. *J. Ceram. Soc. Jpn (Int. Edn)* **96** (1988) 535.
5. JANAF Thermochemical Tables, 3rd edn. American Chemical Society and American Institute of Physics for National Bureau of Standards, Washington 1986.
6. Hendry, A. Thermodynamics of silicon nitride and oxinitride. In *Nitrogen Ceramics*, ed. F. L. Riley. Noordhoff, Leyden, The Netherlands, 1977, p. 183.
7. Itoh, Y., Ishiwata, Y. & Kashiwaga, K., Residual stress characterization of ceramic coatings. *J. Ceram. Soc. Jpn (Int. Edn.)*, **97** (1989) 734.

8 Lange, F F, Compressive surface stresses developed in ceramics by an oxidation induced phase change *J Am Ceram Soc*, **63** (1980) 38

9 Drory, M D & Evans, A G Experimental observations of substrate fracture caused by residually stressed films *J Am Ceram Soc*, **73** (1990) 634

10 Grunninger, M F, Lawn, B R, Farabough, E N & Wachtman Jr, J B, Measurement of residual stresses in coatings on brittle substrates by indentation fracture *J Am Ceram Soc*, **70** (1987) 344

11 Timoshenko, T & Goodier, J N., *Theory of Elasticity*, McGraw Hill, NY 1970, p 433

12 Leng Ward G & Lewis, M. H, Crystallization in Y-Si-Al-O-N glasses *Mat Sci. Eng*, **71** (1985) 101

13 Jack, K H., Review Sialons and related nitrogen ceramics *J Mat Sci*, **11** (1976) 1135

14 Evans, A G & Charles, E A, Fracture toughness determination by indentation *J Am. Ceram Soc*, **59** (1976) 371

15 Lawn, B R & Fuller, E R, Measurement of thin layer surface stresses by indentation fracture. *J Mat Sci*, **19** (1984) 4061

16 Newman, J C & Raju, I S, Stress intensity factor equations for cracks in three dimensional finite bodies In *Proc 14th Symp Fract Mech*, ed J L Lewis & C. Sines. American Society Test Mat, Washington, 1988 p 238

17 Lawn, B R, Evans, A G & Marshall, D B, Elastic/plastic indentation damage in ceramics The medial/radial crack system *J. Am Ceram Soc*, **63** (1980) 574

18 Anstis, G R Chantikul P, Lawn, B R & Marshall, D B, A critical evaluation of indentation techniques for measuring fracture toughness: I Direct crack measurements. *J Am Ceram Soc*, **64** (1981) 533

19 Gillot, L, Cowlam, N & Bacon, G E, A neutron diffraction investigation of some β' sialons *J Mat Sci* **16** (1981) 2263.

20 Hampshire, S, Park, H K, Thompson, D P & Jack, K H, α' Sialon ceramics *Nature* **274** (1978) 880

21 Huang, Z K, Greil, P & Petzow, G, Formation of α Si_3N_4 solid solution in the system Si_3N_4-AlN-Y_2O_3 *Comm. Am Ceram Soc*, **66** (1983) C 96

22 Slasor, S & Thompson, D P Comments on 'Two dimensional solid solution formation of Y containing α Si_3N_4' *J Mat Sci Lett*, **6** (1987) 315.

23 Johnson P M & Hendry A, The microstructure of hot pressed sialon poly types *J Mat Sci*, **14** (1979) 2439

24 Gauckler, L J, Hohnke, H & Tien, T Y, The system Si_3N_4-SiO_2-Y_2O_3 *J Am Ceram Soc*, **63** (1980) 35

25 Dorner, P Gauckler, L J, Krieg, H., Lukas, H L, Petzow, G & Weiss, J, Calculation of heterogeneous phase equilibria in the SiAlON system *J Mat Sci*, **16** (1981) 935

26 Nickel, K G, Hoffmann, M J, Greil, P & Petzow, G, Thermodynamic calculations of the formation of SiC whisker reinforced Si_3N_4 ceramics *Adv Ceram Mat*, **3** (1988) 557

27 Crank, J, *The Mathematics of Diffusion* Clarendon, Oxford, 1967 p 88

28 Matzke, H, Diffusion in carbides and nitrides Unsolved problems *Defect and Diff Forum* **83** (1992) 111

29 Kijama K & Shirasaki, S, Nitrogen self diffusion in silicon nitride *J Chem Phys*, **65** (1976) 2668

30 Raj, R & Morgan, P E D, Activation energies for densification, creep and grain boundary sliding in nitrogen ceramics *Comm Am Ceram Soc.*, **64** (1981) C 143.

31 Angelezio Abantret, F, Pellissier, B, Miloche M & Eveno, P, Nitrogen self diffusion in titanium nitride single crystals and polycrystals *J Eur Ceram Soc*, **8** (1991) 299

32 Kofstad, P, *High Temperature Corrosion* Elsevier, London, 1988

33 Laugier, M T Surface strengthening of ceramics *J Mat Sci. Lett* **5** (1986) 252.

34 Ekstrom T & Nygren, M, Sialon ceramics *J Am Ceram Soc*, **75** (1992) 259

35 Gauckler, L J, Prietzel, S., Bodemer, G & Petzow, G, Some properties of β $Si_{6-z}Al_zO_zN_{8-z}$, In *Nitrogen Ceramics*, Noordhoff, Leyden. The Netherlands, 1977, p 529

36 Tani E, Umebayashi S, Okuzuno, K. Kishi, K & Kobayashi, K, Effect of composition on mechanical properties of β' sialon. *Yogyo Kyokai Shi* **93** (1985) 370

37 Yeheskel, O & Gelen Y The effect of the α phase on the elastic properties of Si_3N_4 *Mat Sci Eng*, **71** (1985)

38 Evans A G & Fu, Y, Microstructural residual stresses. In *Fracture in Ceramic Materials*, ed A G Evans Noyes, Park Ridge, NJ 1984, p 137